



A transcriptome analysis of the antibacterial mechanism of flavonoids from *Sedum aizoon L.* against *Shewanella putrefaciens*

Jing Wang¹ · Zongyu Chi¹ · Ke Zhao¹ · Hongfei Wang¹ · Xin Zhang¹ · Feng Xu¹ · Xingfeng Shao¹ · Yingying Wei¹

Received: 8 April 2020 / Accepted: 13 June 2020 / Published online: 20 June 2020
© Springer Nature B.V. 2020

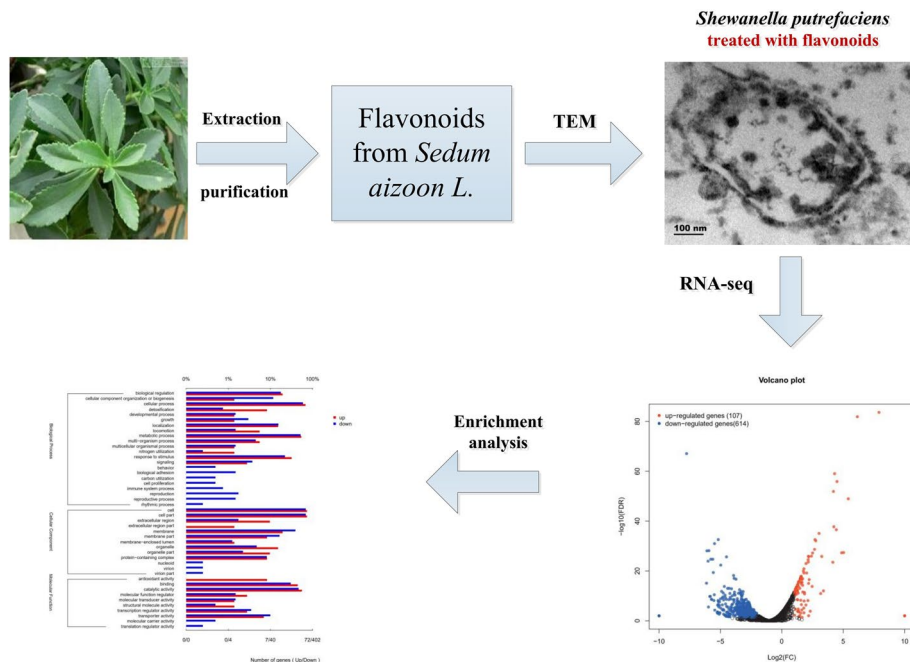
Abstract

Flavonoids from *Sedum aizoon L.* (FSAL) possess prominent antibacterial activity against *Shewanella putrefaciens* isolated from sea food. In the current study, the involved molecular mechanisms were investigated using transcriptome analyses combined with bioinformatics analysis *in vitro* for the first time. Results showed that treatment of FSAL (1.0 MIC) damaged the permeability and integrity of cell membrane and induced 721 differentially expressed genes (DEGs) in tested bacteria at transcriptional levels, including 107 DEGs were up-regulated and 614 DEGs were down-regulated. In addition, the RNA-Seq analysis revealed that the majority of DEGs mainly involved in pathways of lipopolysaccharide biosynthesis, glycerophospholipid metabolism, biosynthesis of amino acids, purine metabolism, ABC transporters and response to stimulus. In summary, the integrated results indicated that the intervention of FSAL induced destruction of cell wall and membrane, disorder of the metabolic process and redox balance, and damage of nucleic acids in *S. putrefaciens*, at last resulted in the death of cells. This study provided new insights into the anti- *S. putrefaciens* molecular mechanism underlying the treatment of FSAL, which may be served as the basis guide for identifying potential antimicrobial targets and application of FSAL in food safety.

Electronic supplementary material The online version of this article (<https://doi.org/10.1007/s11274-020-02871-w>) contains supplementary material, which is available to authorized users.

Extended author information available on the last page of the article

Graphic abstract



Keywords Flavonoids from *sedum aizoon l.* (FSAL) · Antibacterial mechanism · *Shewanella putrefaciens* · Transcriptome

Introduction

Shewanella putrefaciens, a cold-adapted representative of *Shewanella* genus (Fonnesbech et al. 2005) diffusely existed in marine environments (Yang et al. 2017), can induce spoilage presented in chilled seafood products especially fresh shrimp even under modified atmosphere packaging (Mace et al. 2014). Result from its higher microorganism metabolic activity, its biochemical actions can generate hypoxanthine from inosine monophosphate or inosine, produce hydrogen sulfide from cysteine, reduce trimethylamine-N-oxide to trimethylamine (Lyu et al. 2018), and contribute to the proteolytic and lipolytic degradations (Ye et al. 2019), thus the formation of volatile compounds produce unpleasant off-odors (Sae-leaw and Benjakul 2019; Yang et al. 2017). Besides, some strains of *S. putrefaciens* are also assumed to produce tetrodotoxin, one of the neurotoxins as we know (Auawithoothij and Noomhorm 2012). That all leads to decrease the quality of food products. Some recent studies show that *S. putrefaciens* is also relevant to adhesive biofilm formation on abiotic surfaces and seafood products, resulting in persistent contamination (Liu et al. 2017b; Zhang et al. 2016). Hence, it is vital to control safely the growth of *S. putrefaciens* on fresh seafood and other products using innovative antimicrobial techniques.

Flavonoids, as a specific genus of secondary plant metabolites, possesses a wide range of bioactive functions such as anti-oxidation, immune regulation, anticancer and antiviral activities (Georgiev et al. 2014). *Sedum aizoon L.* is regarded as traditional herb widely distributed in China and rich in multiple bioactive constituents including flavonoid, phenolic acid compounds, polysaccharose and alkaloids (Cao et al. 2007; Li et al. 2011; Xu et al. 2015). As a unique natural product, FSAL appears enormous potential in bacteriostatic agent and the antibacterial activities of that against *Staphylococcus aureus*, *Bacillus subtilis* and *Escherichia coli* have demonstrated the study of (Xu et al. 2015) recently. Likewise, our previous research proved the significant effect of FSAL on inhibiting the growth ability of *lactic acid bacteria* and extending refrigerated storage of fresh pork (Xu et al. 2018). However, up to date, no studies have been carried out to investigate the antibacterial activity of FSAL against *S. putrefaciens*, and the antibacterial mechanism of FSAL still need to be further elucidated.

With the rapid development of genome sequencing and genomic technologies, transcriptome enables us to globally investigate the complete responses at a transcriptional level (Chen et al. 2019). As yet, transcription analysis has been applied to explore the antibacterial mechanism of numerous bacteriostats, including natural plant ingredients, antibiotics and nano materials (Petek et al. 2010; Sun et al. 2017).

Therefore, in this study, transcriptomic analyses combined with bioinformatics analysis were conducted for the first time to explore the molecular mechanism of FSAL against *S. putrefaciens* *in vitro*. Differentially expressed genes were identified and then analyzed using Gene Ontology (GO) and Kyoto Encyclopedia of Genes and Genome (KEGG). Further investigations including the changes in characteristics of membrane and production of intracellular ROS were performed to support the sequencing data. These results above provided antibacterial mechanism of FSAL in *S. putrefaciens*, which may be served as the basis for the subsequent study of identifying potential antimicrobial targets to obtain more effective control of this spoilage organism.

Materials and methods

Chemicals and materials

The fresh leaves of *Sedum aizoon L.* were harvested from the experimental field of Ningbo University (Zhejiang Province, China). Nutrient broth (NB) medium was from Guangdong Huankai Microbial Science & Technology Co., Ltd (Guangzhou, Guangdong, China). Quercetin and gallic acid (HPLC grade) were obtained from Shanghai Yuanye Bio-Technology Co., Ltd (Shanghai, China). AB-8 resin and 2,7'-dichloro-fluorescein diacetate (DCFH-DA) were purchased from Solarbio Science & Technology Co., Ltd. (Beijing, China). Distilled water was purified using an ultra-pure water system from Heal Force Instruments (Shanghai, China). All other chemicals and reagents were analytical grade.

Preparation of FSAL

The dried leaves of *Sedum aizoon L.* were prepared and ground into powder using a milling machine, and then passed through a 60-mesh sieve. Briefly, based on our previous experiment (Xu et al. 2018), about 100 g of the powder was extracted with 4 L 70% ethanol at 60 °C for 3 h, homogenized by ultrasonication with a power of 200 W and a frequency of 40 kHz (1 h, 60 °C), then incubated in a 60 °C water bath for 2 h. The extract was concentrated in a vacuum rotary evaporator (Heidolph, Schwabach, Germany). The concentration and double volume of absolute ethanol were placed at 4 °C for 24 h to remove impurities such as protein and polysaccharides. Then the extract was purified using an AB-8 resin. After reaching absorptive saturation, the column was washed by distilled water and then eluted by 80% ethanol. As results, the fractions containing FSAL were concentrated and lyophilized by a freeze-dry system and stored at – 80 °C till further use.

Analysis and characterization of FSAL

The chemical contents of FSAL were determined according to the reported method (Mittal et al. 2013; Zhang et al. 2014) with slight change using high performance liquid chromatography coupled with quadrupole time-of-flight mass spectrometer (HPLC-TOFMS) system (Synapt G2, Waters, USA). Briefly, samples were extracted with methanol: the FSAL was dissolved in HPLC grade methanol and cleared by centrifugation (4500×g, 15 min, 4 °C) for preparing sample solution. The pooled supernatant phases were filtered through 0.22 µm filters for analysis. HPLC analysis was performed on Chromatographic separation was conducted on an Agilent Zorbax XDB-C18 column (4.6×150 mm, 5 µm), samples were injected (10 µL) into the column and eluted at flow rate of 0.8 mL/min. The mobile phase consisted of formic acid solution (0.1%, A) and methanol (B), and elution was performed with a linear gradient as follows: 0–5 min, A from 70 to 30%; 6–18 min, A from 30 to 10%. The temperature of the column oven was set at 25 °C and detection wavelength was 254 nm. ESI-MS analysis was performed in negative ion mode and the operation parameters were as follows: capillary voltage 2.50 kV, skimmer voltage 50.00 V, the temperature of drying gas 250 °C, flow rate of drying gas 6.66 L/min.

Bacterial strains and culture conditions

The bacteria, *S. putrefaciens*, obtained from the BeNa Culture Collection (BNCC, 337021), was kept in food biotechnology laboratory of Ningbo University and maintained in slants of nutrient agar (NA) at 4 °C until required. Nutrient broth (NB) was used for pre-cultivation at 30 °C with aeration and agitation (120 rpm). To obtain a fresh experimental culture, the activated *S. putrefaciens* cells were inoculated in 100 mL of fresh NB medium and incubated at 30 °C in an orbital shaker with 120 rpm till the mid-exponential phase. Then the experimental culture treated with flavonoids from *Sedum aizoon L.* with a final concentration of 2.0 mg/mL was incubated at 30 °C, and bacterial culture with PBS as control. The minimum inhibitory concentration (MIC, 2.0 mg/mL) was determined by standard broth microdilution assay recommended by the Clinical and Laboratory Standards Institute (Diao et al. 2018). Briefly, two-fold serial dilutions of FSAL were prepared in sterile nutrient broth (NB) to a final volume of 100 µL in sterile 96-well microplates. Then, each well was inoculated with 100 µL of cell culture in the logarithmic phase and the final concentration of FSAL was from 0.00 to 16.00 (0.00, 0.25, 0.50, 1.00, 2.00, 4.00, 8.00, 16.00) mg/mL. The plate was incubated at 30 °C for 24 h. MIC was defined as the lowest concentration of FSAL at which the growth of the indicator strain was inhibited completely. MIC determination was conducted in triplicate.

Effect of FSAL on *S. putrefaciens* cell membrane permeability

The effects of FSAL on *S. putrefaciens* cell membrane were investigated by measuring conductivity and the leakage of protein, reducing sugars and nucleic acids. The bacterial culture treated with FSAL (1.0 MIC) was incubated at 30 °C, meanwhile, only the same volume of PBS was added as the control group. The incubated bacteria were taken at various time intervals (0, 1, 2, 3, 4, 5, 6 h) and centrifuged at 2000×g for 10 min. The supernatant was removed and filtered through 0.22 µm membrane. The release of nucleic acids was determined according to the method described by (Cui et al. 2016) with the OD₂₆₀ of each supernatant measured. The concentration of protein and total sugars leakage were obtained based on the method of (Das et al. 2013), with minor modifications. Electrical conductivity was measured as described (Cui et al. 2019) with DDS-307 type conductivity meter.

Transmission electron microscopy (TEM) analysis

The effect of FSAL on microscopic morphologies changes of *S. putrefaciens* was observed using TEM (Liu et al. 2017a). The bacterial culture including the control and FSAL treated were harvested by centrifugation, washed with PBS buffer, subsequently fixed with 2.5% (v/v) glutaraldehyde for 12 h at 4 °C. After being fixed, the samples were rinsed three times in PBS for 15 min at a time and dehydrated with sequential graded cold ethanol (30, 50, 70, and 90%) for 15 min, and ethanol was replaced with anhydrous acetone for 15 min, repeated three times. The specimens were embedded in hard resin after dehydrated and cut into ultra-thin slices (70 nm) using ultramicrotome. The intracellular organization was observed by TEM (H-7650, Hitachi, Japan).

Measurement of ROS production

The production of intracellular ROS detection was analyzed using the fluorescent probe 2,7'-dichlorofluorescein diacetate (DCFH-DA) by confocal laser scanning microscope (CLSM), according to previous reports with some modifications (Ren et al. 2019). The DCFH-DA is non-fluorescent in reduced form and can freely permeates through the cell membrane. Once in the cell, the probe could be hydrolyzed by intracellular esterase to generate DCFH, they are membrane impermeable and trapped inside the cell. When oxidized by ROS, DCFH is converted to the green fluorescing form DCF. Overall, ROS were visualized by fluorescent microplate reader and laser scanning confocal microscope. The bacterial cells were collected till the mid-exponential phase by centrifugation, washed with PBS, re-suspended and mixed thoroughly in presence of 10 µmol/L DCFH-DA

and incubated for 20 min at 37 °C in darkness. To fully remove extracellular DCFH-DA, the cells were washed with PBS for 3 times. Then the bacteria were treated with FSAL (1.0 MIC) and the same volume of PBS for 1 h and 3 h at 30 °C. The intracellular ROS values were captured using CLSM (LSM880, Zeiss, Germany) and reported fluorescence intensity.

RNA preparation, library construction and sequencing

The bacterial cells (10⁸ CFU/mL) for RNA-seq analysis were collected 3 h after the addition of FSAL (1.0 MIC), at the same time, only the same volume of PBS was added as the control group. After centrifugation at 14,000×g at 25 °C for 1 min, the supernatant was discarded, then the bacterial pellet was frozen in liquid nitrogen for 4 h and stored at -80 °C. All treatments were performed in triplicate.

Total RNA was isolated from each sample using the TRIZOL, after extraction, mRNAs were enriched by oligo magnetic beads. Then, for purpose of maximizing the diversity of transcriptional units, the high-quality RNA of 5.0 µg from each sample were mixed into a single large pool. The library construction and the RNA-seq were performed by LC-Bio Technology Co., Ltd., Hang Zhou, Zhejiang Province, China. In general, mRNA was broken into small pieces in fragmentation buffer. RNA fragments were reverse-transcribed to create the final cDNA library using the Truseq™ Stranded RNA sample prep Kit (Illumina, San Diego, USA). The fragments were copied into first strand cDNA using random primers subsequently the second strand cDNA synthesis was performed. The dUTP was used to instead of dTTP for the second strand synthesis, and the index adapters were connected by the Truseq™ Stranded RNA sample prep Kit. Then agarose gel electrophoresis was used to separate and selected fragments and the final sequencing library was acquired by means of PCR amplification. Finally, the paired-end (2×150 bp) sequencing was performed on the Illumina HiSeq™ 4000 sequencing platform.

Reads mapping, annotation and analysis

The transcriptome was sequenced by the approach of Illumina paired-end RNA-seq, and a total of million paired-end reads of bp length were generated. To get high-quality data and ensure the accuracy of subsequent biological information analysis, the trimming adapters and removing low-quality sequencing were used to filtered the raw reads. Preparation before assembly, the low-quality reads including reads contained sequencing adaptors, reads contained sequencing primer and nucleotides with q quality values <20 were discarded. Genes were determined to have different gene expression significantly with ratio changed > twofold with

$q < 0.05$. Besides, in order to eliminate the effect of sequencing artifacts, 75 bp was the minimum acceptance length. The ratios were reported as the up- or down-fold change.

With the analysis of pathway tools, annotation of genes was used to predict biochemical pathways. GO (Gene Ontology) and KEGG (Kyoto Encyclopedia of Genes and Genomes) pathways were retrieved respectively from GO (<https://geneontology.org>) and KEGG web server (<https://www.kegg.jp/kegg>).

Defining and analysis of differentially expressed genes

We evaluated the repeated correlation of samples in order to compare gene expression levels in different libraries. To eliminate the effect of differences in gene length and sequencing quantity on calculating gene expression, Reads per Kilobase of Transcript per Million Reads Mapped (RPKM) was used to calculate and normalize the transcript level of each expressed gene. Differentially expressed genes (DEGs) under FSAL treatment were identified as genes with the combined selection standard of fold change (FC) ≥ 2 and a Chi square test (FDR < 0.05).

Quantitative real-time PCR validation

In order to evaluate the validity of Illumina analysis, real-time PCR assay was conducted on *S. putrefaciens* treated with the same method used in RNA-Seq. Ten DEGs were selected from different pathways to confirm the RNA-Seq results and the relative expression level of the genes was calculated with the $2^{-\Delta\Delta CT}$ method after normalization, 16S rRNA was used as the internal reference (Liu et al. 2020).

Statistical analysis

All experiments were conducted in triplicates and statistical analysis was performed using the SPSS package program version 19.0 (SPSS Inc., Chicago, IL, USA). Obtained results of comparison between groups were analyzed using one-way analysis of variance (ANOVA). Duncan's multiple range tests were applied to determine the significant differences with the level of $P < 0.05$.

Results

Chemical compositions of FSAL

Composition analysis of FSAL was shown in Table 1, as can be seen from the study, quercetin was the major components of FSAL we prepared, followed by gallic acid. The relative

Table 1 The analysis of the chemical contents of flavonoids from *Sedum aizoon L*

Name of components	Retention time (min)	Molecular weight	Content (mg/g)
Quercetin	8.07	447.09	171.07 \pm 11.34
Gallic acid	2.26	169.02	159.22 \pm 9.07

contents, retention time and other characterizations of the individual constituent was presented in the results.

Effect of FSAL treatment on *S. putrefaciens* cell membrane permeability

To analyze cell membrane permeability, the electrical conductivity, protein concentration, sugar concentration and nucleic acids content of the bacterial culture were determined. As shown in Fig. 1a, the constant increase in electrical conductivity was seen in FSAL-treated samples with passage of time, which had significant differences in comparison with the control. The data indicated that some molecules such as Na^+ , K^+ in the cell were leaked due to the addition of FSAL. The protein concentration in suspension of FSAL-treated bacterial culture had a violent rise in the first three hours, and still increased afterwards (Fig. 1b). However, in contrast, that in the control solution did have no significant differences observed as time went by. During the culture period, the sugars concentration in both FSAL-treated and the control samples increased over 6 h time course (Fig. 1c). Meanwhile, after treatment with FSAL, the content of sugars released from cells was markedly higher than the control. Compared with untreated tests, the absorbance value of extracellular nucleic acids of cells had pronounced growth in the first five hours then decreased thereafter (Fig. 1d). However, only little change was observed in control samples. The above results demonstrate that FSAL may profoundly enhance the cells membrane permeability of *S. putrefaciens* and destroy the membrane structure, causing leakage of intracellular components, thereby affecting the normal physiological metabolism of the cells.

TEM analysis of *S. putrefaciens* treated with FSAL

The influence of FSAL on the intracellular organization of *S. putrefaciens* was observed with TEM. According to Fig. 2a, the intracellular organization of cells from control samples exhibited clear and normal morphology, plump and uniform distribution of cytoplasm and distinct integrity of membranes. In contrast, following treatment with FSAL for 3 h, the ultrastructure of cells was irregularly shaped and disorganized. As shown in Fig. 2b, intracellular structural damage, loss of cytoplasm, discontinuity of membranes and

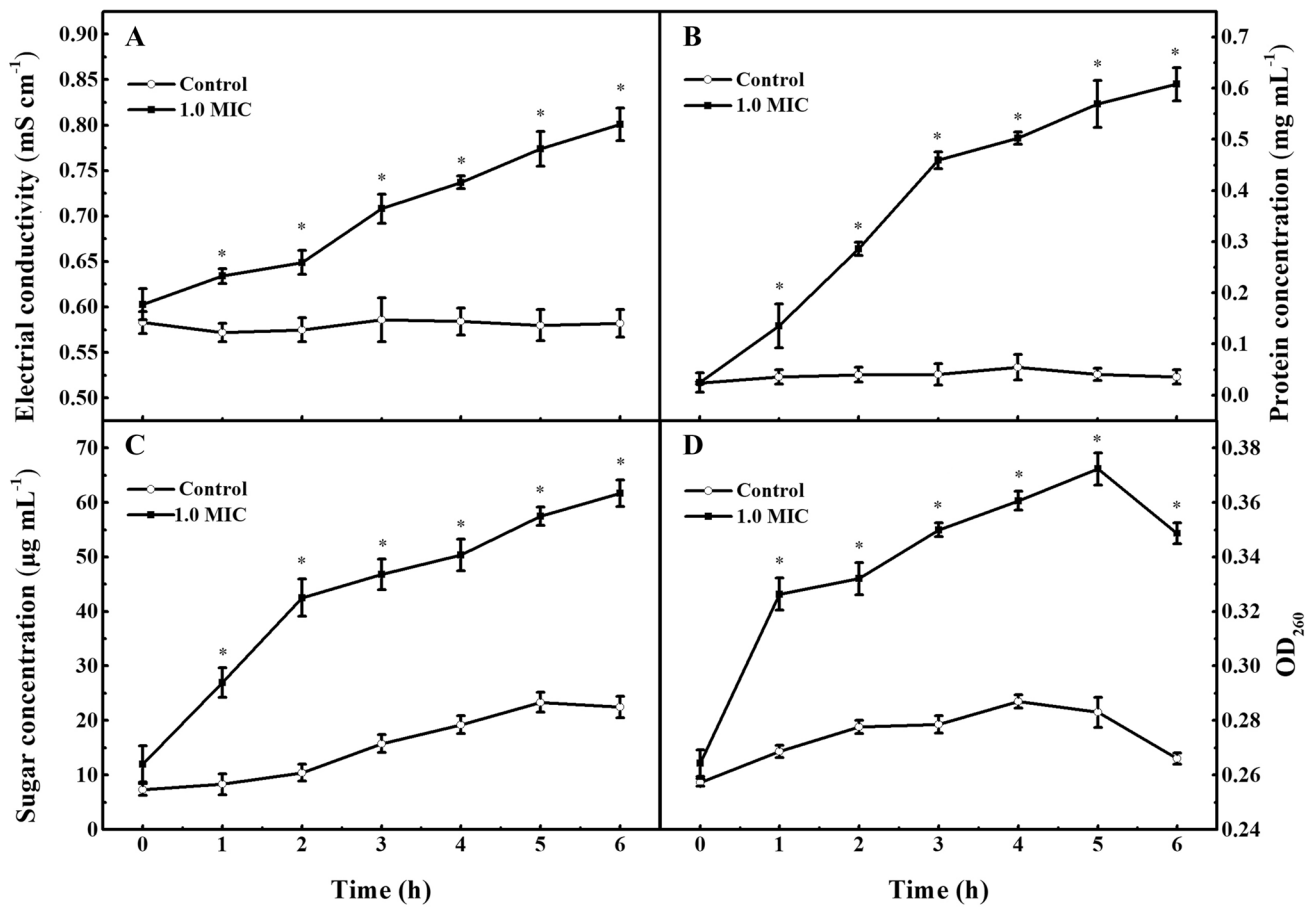


Fig. 1 The effects of FSAL (1.0 MIC) on *S. putrefaciens* cell membrane permeability, and the control group was treated with PBS. The electrical conductivity (a), protein concentration (b), sugar concentration (c) and nucleic acids content (d) of the bacterial culture. Each data in the figures represents the mean \pm standard error of three rep-

licate samples. Vertical bars represent standard errors of the means. Asterisks indicate significant differences between FSAL-treated and control samples. The data were analyzed by one-way analysis of variance (ANOVA), * $P < 0.05$

rupted cell surface were detected. In addition, the destruction of cytoplasmic organization increased with longer processing time. After 6 h of exposure to FSAL, cell structure was further disrupted (Fig. 2c). Due to loss of cytoplasmic components, the lower density of cells was presented, furthermore, vacuolization and cell debris were also emerged under FSAL-treated. Based on ultrastructure analysis, the results of TEM demonstrate that the mechanism of FSAL against *S. putrefaciens* involves the destruction of cell membrane integrity lead to release of cellular contents and cell death.

Effect of FSAL treatment on intracellular ROS level in *S. putrefaciens* cells

The fluorescent probe DCFH-DA was used to detect intracellular ROS, a key factor associated with apoptosis, in *S. putrefaciens* cells treated with FSAL at 1.0 MIC. DCFH-DA is oxidized to DCF by intracellular ROS, leading to

the increase of fluorescence intensity. As shown in Fig. 3, in our study, the intracellular ROS level in *S. putrefaciens* cells from the control samples had not changed much. On the contrary, after exposing to FSAL, the green fluorescent signal was enhanced in cells. Meanwhile, the accumulation of intracellular ROS dramatically increased as time went on (Fig. 3b, d, f). The result indicates that ROS are produced in *S. putrefaciens* strains treated with FSAL. Also, ROS enhancement provides oxidative stress sharply and promotes cell damage of *S. putrefaciens*.

Library construction and RNA-sequencing data

The libraries representing transcriptome of FSAL-treated samples and control samples were constructed for RNA-seq respectively. Absolutely, after getting rid of reads with adaptor contamination, insufficient length, or unacceptable sequencing of low-quality base scores, the clean data of two groups were obtained with average quality values ≥ 30 for

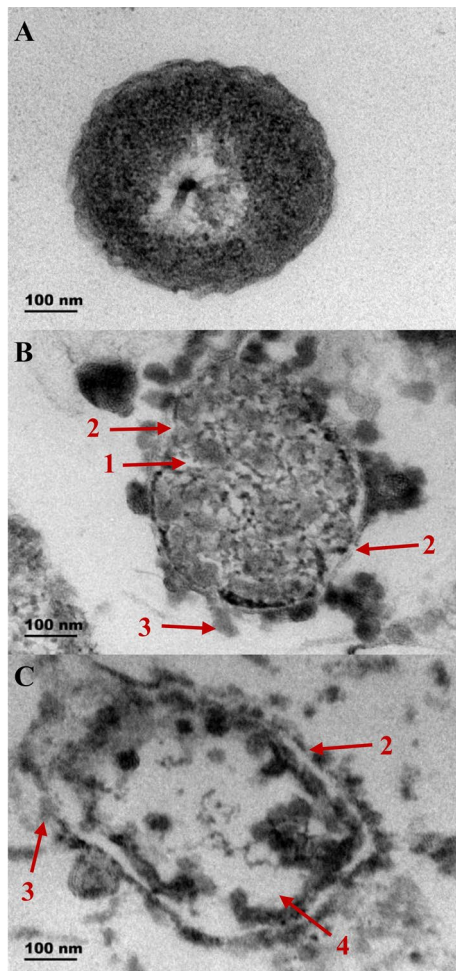


Fig. 2 Effect of FSAL on the ultrastructure of *S. putrefaciens*. **a** TEM images of cells untreated (control); **b** TEM images of cells treated with FSAL (1.0 MIC) for 3 h; **c** TEM images of cells treated with FSAL (1.0 MIC) for 6 h. Intracellular structural damage and loss of cytoplasm (arrows #1), discontinuity and ruptured cell surface (arrows #2), cytoplasm material leaked around cell surrounding (arrows #3) as well as vacuolization (arrows #4) were visible

more than 94.83% of the reads (Table S1). The results of quality screened reads aligned and mapped to *S. putrefaciens* reference genome using Rockhopper shown that more than 80.72% of reads in FSAL-treated libraries and 79.16% in control were matched to *S. putrefaciens* genes, suggesting successful library construction and RNA sequencing.

Identification of DEGs

According to comparative transcriptomic results, FSAL treatment induced significant changes in *S. putrefaciens* at the mRNA level, indicating a molecular mechanism. Gene expression levels were calculated using FPKM values. As shown in Fig. 4, totally, 721 DEGs were identified in samples with FSAL stress, of which, 107 DEGs were up-regulated

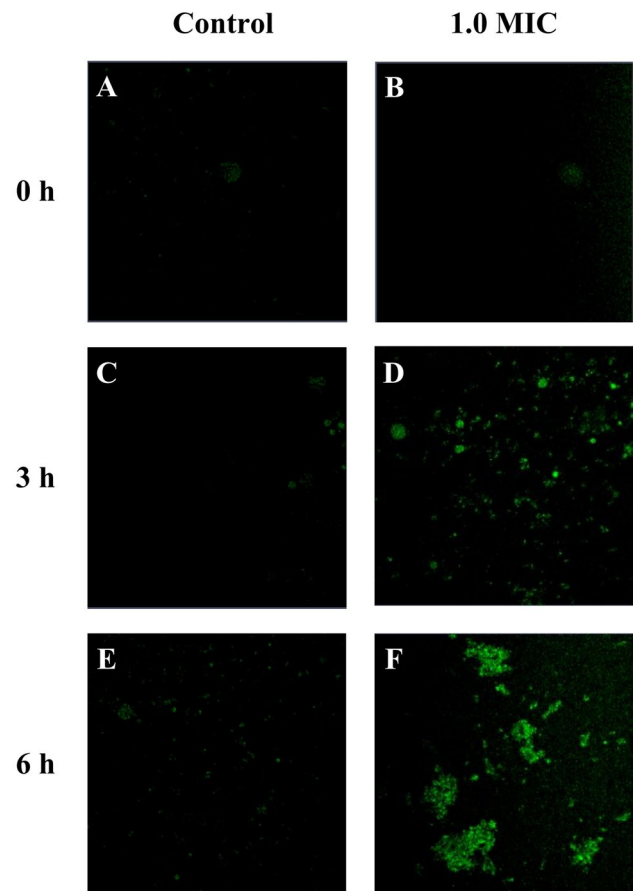


Fig. 3 Effects of FSAL (1.0 MIC) treatment on intracellular ROS level in *S. putrefaciens* cells, and the control group was treated with PBS. Intracellular ROS level of cells from control group (**a**, **c**, **e**); intracellular ROS level of cells treated with FSAL at 1.0 MIC for 0 h (**b**), 3 h (**d**) and 6 h (**f**)

and 614 DEGs were down-regulated in comparison with the control group. Table S2 showed description detailed of DEGs between the FSAL-treatment and the control groups.

GO classification analysis

Based on the data, in order to gain insight into the functional categories of the DEGs after FSAL intervention, as presented in Fig. 5, DEGs annotated by GO enrichment analysis were classified into three categories of biological process (BP), cellular component (CC) and molecular function (MF), which were composed of 22, 13 and 10 subcategories, respectively. Within the category of BP, the DEGs were mainly distributed in cellular process, metabolic process, response to stimulus and biological regulation. While for the GO functions of CC category, cell, cell part, membrane and membrane part constituted the most abundant components. With regard to MF category, the main groups that DEGs mostly located in were catalytic activity, binding and

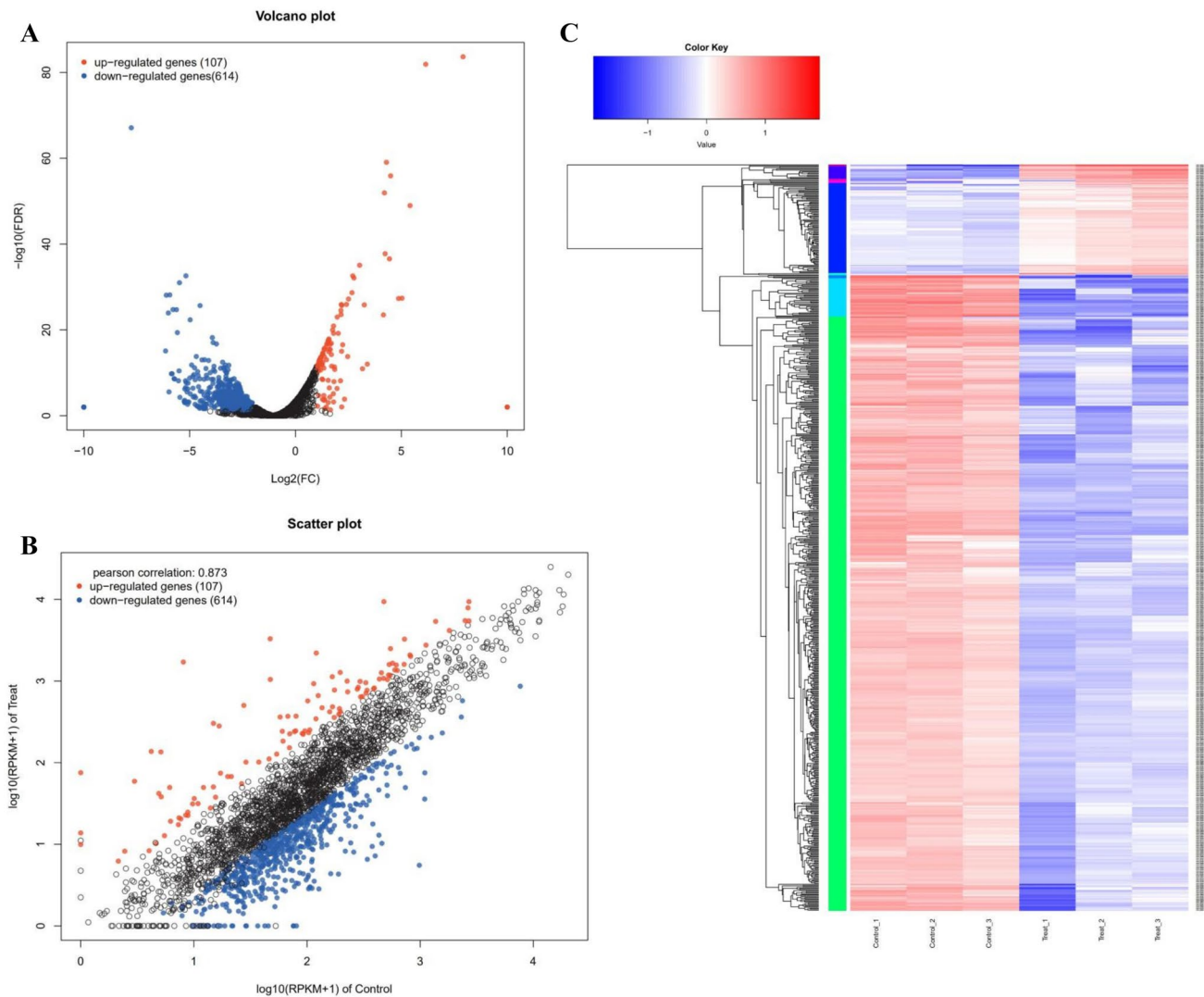


Fig. 4 Distribution of DEGs in FSAL-treated and control *S. putrefaciens*. **a** Visualization volcano-plots of DEGs. Each dot represents a gene, red dots (significantly up-regulated genes), blue dots (significantly down-regulated genes) and black dots (non-significantly different genes) for each group indicated on the diagram. **b** Visualization

scatter-plots of DEGs. Colors are as in (a). **c** Heatmap showing all DEGs. Colors demonstrate expression level patterns in FSAL-treated and control groups. Red cluster represents up-regulated expression and blue cluster represents down-regulated expression

transporter activity. Table S3 showed the specific description and characteristic of DEGs respectively of BP, CC and MF. In conformity to GO enrichment analysis, the results indicated that the majority of DEGs were found in cell periphery (174 DEGs), plasma membrane (151 DEGs) and membrane (172 DEGs) locations. (Table S3) The results of GO classification between the control and FSAL-treated group showed that FSAL stress obviously affected several membrane functions and major biological processes for *S. putrefaciens*.

KEGG pathway analysis

To obtain further systematical analysis of the DEGs functions, KEGG pathways significant enrichment analysis,

which were tested using KOBAS, was performed to categorize DEGs into different pathways based on bioinformatic databases. As shown in Fig. 6 and Table S4, the results indicated that DEGs were significantly involved in pathway of ABC transporters, flagellar assembly, glycerophospholipid metabolism and two-component system. Moreover, based on the analysis of the data shown in Table S5, DEGs up-regulated by exposure to FSAL were mostly located in pathways of glyoxylate and dicarboxylate metabolism, microbial metabolism in diverse environments, flagellar assembly and carbon metabolism. While DEGs down-regulated were related to biosynthesis of amino acids, lipopolysaccharide biosynthesis, homologous recombination, purine metabolism, biosynthesis of

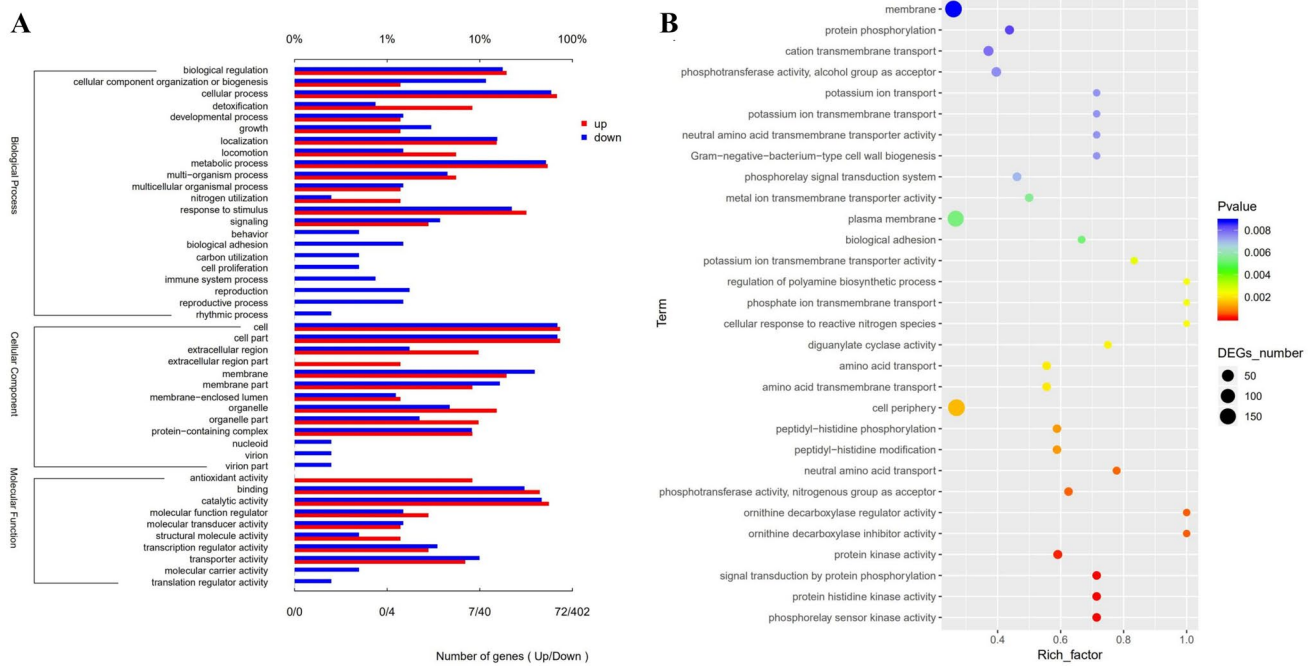


Fig. 5 GO analysis of DEGs between FSAL-treated and control group. **a** Histogram of GO (biological process, cellular component and molecular function) annotation of DEGs. **b** GO enrichment analysis of DEGs

secondary metabolites, metabolic pathways, two-component system and ABC transporters.

RNA-Seq expression validation by quantitative real-time PCR

In order to evaluate the validity of the RNA-Seq data, RT-qPCR assay was used to determine the expression of DEGs with the same RNA samples. The results of DEGs tested were generally in conformity to RNA-Seq results, suggesting that the RNA-Seq results were valid.

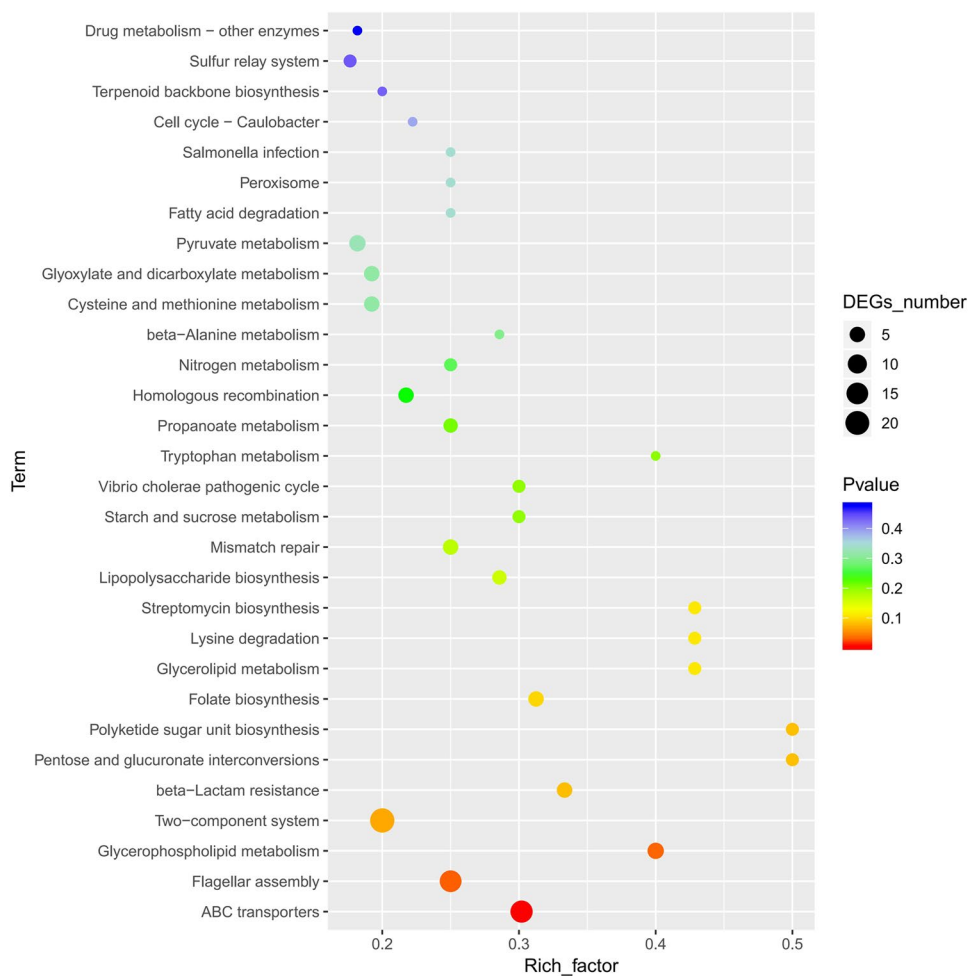
Discussion

Cell wall and membrane

As protective barrier to maintain bacterial cell integrity and shape, the cell wall of *S. putrefaciens* are composed of peptidoglycan, lipopolysaccharide, lipid bilayer and lipoprotein (Brown et al. 2015). Some reports have revealed that the disruption of the cell wall structure has a great impact on the survival of bacterial cells, causing the plasma membrane rupture and cell lysis (Gomes et al. 2020). Composed of phospholipid bilayer and protein, bacterial cell membranes are rich in enzymes that perform many important metabolic functions, including nutrients uptake, homeostasis and the enzyme system contained electron transfer and oxidative

phosphorylation, which has some functions of mitochondria (Luo et al. 2014). Thus, even relatively slight changes to the structural integrity of cell membranes can hurtfully influence on cell functions and result in cell death (Yi et al. 2018). In order to elucidate the antibacterial mechanisms of flavonoids, numerous investigators have begun to study the influence of cell wall and membranes under flavonoids treatment (Xu et al. 2018). Hence, as a general phenomenon results in cell death, leakage of intracellular material (Fig. 1) and microscopic morphologies changes (Fig. 2) were investigated in the first of present study to determine effect of FSAL on cell wall structure and membrane permeability. The bacterial plasma membrane supplied a permeability barrier to the passage of small ions such as Na^+ , K^+ , which is maintained and regulated by the chemical compositions and structural of the membrane itself (Xiang et al. 2018). The stabilization of necessary electrolytes could maintain proper enzyme activity and promote cell membrane functions, including regulation of metabolism, solute transport, control of turgor pressure and motility (Li et al. 2014). However, remarkable increases in the leakage of ions in FSAL-treated group indicated a disruption of this permeability barrier. Furthermore, compared with the control group, we also found that FSAL caused markedly rapid efflux of cytoplasm material from *S. putrefaciens*, including protein, nucleic acid and total sugars, which play an important role in many metabolic processes. And they were used as indicators of rough and irreversible damage to the cytoplasmic

Fig. 6 KEGG analysis of DEGs between the control and FSAL-treated group



membrane and inhibition of cell survival (Shen et al. 2015). Consistent with these results, Our TEM observations of *S. putrefaciens* treated with FSAL decidedly confirmed severe morphological changes even breakdown in structure of the cell wall and membrane. Similar effects were found in phenols and terpenes (Churklam et al. 2020), which exerted their antimicrobial action closely associated with increasing membrane permeability and eventually induced the death of bacterial cell.

Transcriptome analysis was used in the rest of present study to explore the molecular mechanism of FSAL against *S. putrefaciens* in cell structure. Indeed, based on the results, cell wall and membrane of *S. putrefaciens* were pretty affected by FSAL treatment. Firstly, according to bioinformatics analysis, the most DEGs were associated with cell wall and membrane. Secondly, the result showed that the genes involved in cell wall structure were significantly differentially expressed in response to FSAL treatment. Compared with the control group, significantly down-regulated genes in the FSAL-treat group related to cell wall component included *RS02590*, *RS04160*, *RS04545* and *RS05150* for lipopolysaccharide biosynthesis. In addition,

as well as DEGs (*RS13125* and *RS16010*) for peptidoglycan biosynthesis. As essential ingredient of Gram-negative bacterial cell wall structure, lipopolysaccharide hedges the penetration of antimicrobial components and stimulates the immune function of cell. And the previous study has reported that peptidoglycan biosynthesis was required for cell division and regarded as the targets of antibacterial drug (Brown et al. 2015). Furthermore, in comparison with the control, present study showed that membrane related DEGs *RS03115*, *RS06440* and *RS14755* for glycerolipid metabolism, *RS03115*, *RS14755*, *RS13665*, *RS03685*, *RS06440* and *RS05190* for glycerophospholipid metabolism, *RS19365* for biosynthesis of unsaturated fatty acids, *RS04740* for saturated fatty acid biosynthesis, *RS16965* for inositol phosphate metabolism and others for encoding membrane protein (15 DEGs for ABC transporters) were significantly down-regulated. At the same time, we also found that *RS04980*, *RS16585* and *RS19435* for butanoate metabolism related to maintain the integrity of membrane and *RS11765* for RND transporter regarded as major drug efflux pumps in many Gram-negative bacteria were up-regulated expressively. It suggested that cells have begun to adjust their physiology

in response to adverse changes around environment. Membrane proteins are responsible for various functions, including nutrient transport, response to environmental stress, biofilm formation and antibiotic resistance (Li et al. 2015; Nakayama et al. 2013). In addition, as one part of them, known for their capability of translocating diverse molecules across cellular membranes in an ATP-dependent manner, ABC transporters are a ubiquitous class of membrane integral efflux transporters. It has also been extensively studied in the past few years about ABC transporters from bacteria (Rees et al. 2009), and numerous DEGs for ATPase activity and transmembrane movement of substances were identified. Therefore, that would be connected to the disruption to transmembrane transport and capacity of using energy of hydrolyzed ATP of cells following FSAL treatment. As we known, phospholipids are importantly principal component of cell membranes, and phosphatidic acid is the key precursor of phospholipid biosynthesis (Lin et al. 2018). Interestingly, it has been studied that, after intervention with morusin (Pang et al. 2019), expression of phosphatidic acid biosynthesis-associated genes was down-regulated significantly. Indeed, fatty acids are the materials for synthesis of phosphatidic acids (Luo et al. 2014) and our data has shown that genes associated with both unsaturated fatty acids biosynthesis and saturated fatty acids biosynthesis pathway were affected after exposing to FSAL. These results indicate that FSAL has potent antibacterial influence on regulation of phospholipids and fatty acid biosynthesis pathway to inhibit the membrane-repair system. Overall, combined with the above analysis, the possible antibacterial mechanisms describing the effect of FSAL on *S. putrefaciens* involves affecting the protein composition, decreasing synthesis of essential compound required and disrupting integrity and structure of cell wall and membrane.

Amino acid metabolism

Beyond the damage of cell wall and membrane, according to various DEGs related to metabolism process in the present study, *S. putrefaciens* also underwent metabolism process limitation in the presence of FSAL. Amino acids are the major metabolites involved in the biosynthesis and metabolism of *S. putrefaciens*. As shown in Table S5, the expressions of many membrane proteins associated with the influx of essential amino acids for bacteria were decreased, which lead to reduce uptake of extracellular nutrients like amino acids. Meanwhile, with uptake limitation of amino acids, previous reports stated that bacteria in turn regulated genes related to synthesis and metabolism of amino acids (Horinouchi et al. 2010; Liu et al. 2020). Under the stimulus of FSAL, *RS00975* and *RS16585* for tyrosine metabolism, *RS04980* and *RS10320* for tryptophan metabolism, *RS00975* and *RS19475* for cysteine and methionine metabolism,

RS03990, *RS10335* and *RS16585* for alanine, aspartate and glutamate metabolism were over-expressed. On the contrary, *RS01620*, *RS06125*, *RS09215*, *RS13160* and *RS16965* for biosynthesis of amino acids, *RS03630*, and *RS15865* for arginine and proline metabolism *RS01620*, *RS06125* and *RS13160* for phenylalanine, tyrosine and tryptophan biosynthesis were significantly down-regulated. Interestingly, it has also shown that bacterial cells commonly activated biosynthetic pathways of some amino acids for survival after several stress treatments (Liu et al. 2020). Nonetheless, the activation of these biosynthetic pathways also resulted in excessive consumption of several specific amino acids. That indicates that an unbalanced state and metabolism disturbance of amino acids in the cell was produced when treated with FSAL. Therefore, combined with the above considerations, the present study implies that FSAL treatment reduced extracellular amino acid uptake, and then compelled *S. putrefaciens* cells to acquire several amino acids from intracellular biochemical processes, thus leading to metabolism disturbance and consequently inhibit survival of *S. putrefaciens* cells.

Oxidative phosphorylation and ROS

In this study, three significantly down-regulated genes (*RS11015*, *RS11050* and *RS11225*) involved in oxidative phosphorylation were observed in the FSAL-treated group. Oxidative phosphorylation, an intracellular biochemical process, enables the build-up of a proton gradient and ultimately leads to the conversion of ADP to ATP when substance is oxidized. Due to its important part in meeting the energy needs of bacterial survival, oxidative phosphorylation has emerged as major target pathway of new drugs within the last decade. Interestingly, in the case of nutrient deficiency or external stimulation, bacteria have to reduce their metabolic level of oxidative phosphorylation to adapt to the stressful environment they are in (Antonenko et al. 2017). It suggested that FSAL treatment induced energy metabolism disorder and was regarded as a threat against survival of *S. putrefaciens* cells. In addition, reactive oxygen species (ROS) are an evitable side product of oxidative phosphorylation and considered as intracellular apoptotic factors in bacteria. It was previously described that external stimulus could induce intracellular ROS production and the primary targets are thought to promote the oxidation of nicotinamide adenine dinucleotide (NADH) through the electron transport chain (Huang et al. 2018). In the present study, the accumulation of intracellular ROS dramatically produced in *S. putrefaciens* strains treated with FSAL (Fig. 3), and transcriptome analysis showed that 6 DEGs associated with detoxification, 6 DEGs related to antioxidant activity and 23 DEGs involved in response to stimulus were up-regulated. Particularly, antioxidant defense systems (*RS14135* for thioredoxin TrxA, *RS10320* for peroxidase, *RS13500* for superoxide

dismutase, *RS00400* for cytochrome-c peroxidase, *RS07550* for peroxiredoxin and *RS05455* for glutathione peroxidase were over expressed) was stimulated under oxidative stress produced by FSAL treatment. Meanwhile, previous study has reported that the production of intracellular ROS caused serious cellular damage, lipid peroxidation lead to degradation of the membrane structures of cells, protein peroxidation resulted in metabolism disorder, and DNA breaks (Ren et al. 2019). Thus, it can be inferred that FSAL treatment can give rise to disorder of energy metabolism and imbalance of redox state in *S. putrefaciens* strains.

DNA replication and repair system

Another possible antimicrobial mode of FSAL was associated with 260-nm absorbing materials included DNA and RNA (nucleic acids), which are the key structural components in the cytoplasm (Ning et al. 2017). As we known, folate regarded as methyl donors plays an important part in the synthesis of DNA nucleotides such as thymine. In this study, DEGs (*RS02440*, *RS02810*, *RS06430*, *RS06435* and *RS15655*) involved in folate biosynthesis were down-regulated in the FSAL-treated group. Therefore, it suggests that FSAL treatment can bring folate deficiency to *S. putrefaciens* cells and then lead to damage of nucleic acids. In addition, under FSAL stress, the DNA replication and repair system is more important to the survival of *S. putrefaciens* cells. According to the results of transcriptome analysis, there are many down-regulated DEGs encoding proteins involved that system, mainly containing 5 DEGs for homologous recombination, 3 DEGs for pyrimidine metabolism, 2 DEGs for DNA replication and 8 DEGs for purine metabolism. Particularly, the two down-regulation of DEGs (*RS00770* and *RS16795*) participating in DNA polymerase subunits and the over expression of *RS13860* encoding nucleoside phosphorylase were also observed with FSAL intervention. Thus, it implies that FSAL may destroy the processes of DNA replication, repair, and recombination in *S. putrefaciens*. Similar to our results, a previous study expounded profoundly that action of antibacterial agent might result in generating double-stranded DNA breaks trapped by covalently-linked topoisomerases and then destroy its function (Kang et al. 2020). In summary, as a result of exposure to FSAL, replication machinery and synthesis of DNA was restrained, which leads to inhibit protein biosynthesis and metabolism, eventually cell death.

Conclusions

The study makes use of transcriptome combined with bioinformatics analysis for the first time to obtain an insight into the antibacterial mechanism of FSAL against *S. putrefaciens*.

The results showed that FSAL intervention caused damage permeability and integrity of cell membrane, increased dramatically concentration of intracellular ROS and induced significant changes in numerous genes. For GO enrichment analysis, the DEGs were mainly distributed in membrane functions, metabolic process and response to stimulus. Meanwhile, KEGG pathways analysis indicated that DEGs were mostly involved in pathway of ABC transporters, glycerophospholipid metabolism, biosynthesis of secondary metabolites and two-component system. Thus, the results revealed that FSAL has obvious antibacterial effects that disrupt the structural integrity of cell wall and membranes and detrimentally influence the metabolism process to disturb cellular functions, and result in cell death. The above results provided theory basis for the antibacterial mechanisms of FSAL, which may promote the guide for exploitation and applications of FSAL and other plant-derived bacteriostats in food-related preservation technology.

Acknowledgements This study was supported by Public Welfare Project of Zhejiang Province (LGN19C200012), Natural Science Foundation of Zhejiang Province (LY16C200003), Natural Science Foundation of Ningbo City (2015A610273) and Key Research and Development Projects of Zhejiang Province (2017C02021).

Compliance with ethical standards

Conflicts of interest The authors have declared no conflict of interest.

References

- Antonenko YN, Denisov SS, Khailova LS, Nazarov PA, Rokitskaya T, Tashlitsky VN, Firsov AM, Korshunova GA, Kotova EA (2017) Alkyl-substituted phenylamino derivatives of 7-nitrobenz-2-oxa-1,3-diazole as uncouplers of oxidative phosphorylation and antibacterial agents: involvement of membrane proteins in the uncoupling action. *Biochim Biophys Acta Biomembr* 1859:377–387
- Auawithoohitij W, Noomhorm A (2012) *Shewanella putrefaciens*, a major microbial species related to tetrodotoxin (TTX)-accumulation of puffer fish *Lagocephalus lunaris*. *J Appl Microbiol* 113:459–465
- Brown L, Wolf JM, Prados-Rosales R, Casadevall A (2015) Through the wall: extracellular vesicles in Gram-positive bacteria, mycobacteria and fungi. *Nat Rev Microbiol* 13:620–630
- Cao X, Li S, Wang C, Lu M (2007) Potential use of the herbicide quizalofop-*p*-ethyl for eicosapentaenoic acid overproduction by the diatom *Nitzschia laevis*. *Chin J Biotechnol* 23:885–890
- Chen Y, Cheng L, Zhang X, Cao J, Wu Z, Zheng X (2019) Transcriptomic and proteomic effects of (–)-epigallocatechin 3-*O*-(3-*O*-methyl) gallate (EGCG3"Me) treatment on ethanol-stressed *Saccharomyces cerevisiae* cells. *Food Res Int* 119:67–75
- Churklam W, Chaturongakul S, Ngamwongsatit B, Aunpad R (2020) The mechanisms of action of carvacrol and its synergism with nisin against *Listeria monocytogenes* on sliced bologna sausage. *Food Control* 108:106864
- Cui H, Ma C, Li C, Lin L (2016) Enhancing the antibacterial activity of thyme oil against *Salmonella* on eggshell by plasma-assisted process. *Food Control* 70:183–190

- Cui H, Zhang C, Li C, Lin L (2019) Antibacterial mechanism of oregano essential oil. *Ind Crop Prod* 139:111498
- Das MR, Sarma RK, Borah S, Kumari R, Saikia R, Deshmukh AB, Shelke MV, Sengupta P, Szunerits S, Boukherroub R (2013) The synthesis of citrate-modified silver nanoparticles in an aqueous suspension of graphene oxide nanosheets and their antibacterial activity. *Colloid Surf B Biointerfaces* 105:128–136
- Diao M, Qi D, Xu M, Lu Z, Lv F, Bie X, Zhang C, Zhao H (2018) Antibacterial activity and mechanism of monolauryl-galactosylglycerol against *Bacillus cereus*. *Food Control* 85:339–344
- Fonnesbech VB, Venkateswaran K, Satomi M, Gram L (2005) Identification of *Shewanella baltica* as the most important H₂S-producing species during iced storage of Danish marine fish. *Appl Environ Microbiol* 71:6689–6697
- Georgiev V, Ananga A, Tsolova V (2014) Recent advances and uses of grape flavonoids as nutraceuticals. *Nutrients* 6:391–415
- Gomes TA, Zanette CM, Spier MR (2020) An overview of cell disruption methods for intracellular biomolecules recovery. *Prep Biochem Biotechnol* 19:1–20
- Horinouchi T, Tamaoka K, Furusawa C, Ono N, Suzuki S, Hirasawa T, Yomo T, Shimizu H (2010) Transcriptome analysis of parallel-evolved *Escherichia coli* strains under ethanol stress. *BMC Genomics* 11:579
- Huang Z, He K, Song Z, Zeng G, Chen A, Yuan L, Li H, Hu L, Guo Z, Chen G (2018) Antioxidative response of *Phanerochaete chrysosporium* against silver nanoparticle-induced toxicity and its potential mechanism. *Chemosphere* 211:573–583
- Kang S, Kong F, Shi X, Han H, Li M, Guan B, Yang M, Cao X, Tao D, Zheng Y, Yue X (2020) Antibacterial activity and mechanism of lactobionic acid against *Pseudomonas fluorescens* and methicillin-resistant *Staphylococcus aureus* and its application on whole milk. *Food Control* 108:106876
- Li W, Luo Q, Wu L (2011) Two new prenylated isoflavones from *Sedum aizoon L.* *Fitoterapia* 82:405–407
- Li Y, Han Q, Feng J, Tian W, Mo H (2014) Antibacterial characteristics and mechanisms of ε-poly-lysine against *Escherichia coli* and *Staphylococcus aureus*. *Food Control* 43:22–27
- Li YQ, Sun XX, Feng JL, Mo HZ (2015) Antibacterial activities and membrane permeability actions of glycyl-L-histidyl-L-threonine against *Escherichia coli*. *Innov Food Sci Emerg Technol* 31:170–176
- Lin Y, Bogdanov M, Lu S, Guan Z, Margolin W, Weiss J, Zheng L (2018) The phospholipid-repair system LplT/Aas in Gram-negative bacteria protects the bacterial membrane envelope from host phospholipase A₂ attack. *J Biol Chem* 293:3386–3398
- Liu G, Ren G, Zhao L, Cheng L, Wang C, Sun B (2017a) Antibacterial activity and mechanism of bifidocin A against *Listeria monocytogenes*. *Food Control* 73:854–861
- Liu J, Yu S, Han B, Chen J (2017b) Effects of benzalkonium chloride and ethanol on dual-species biofilms of *Serratia liquefaciens* S1 and *Shewanella putrefaciens* S4. *Food Control* 78:196–202
- Liu M, Feng M, Yang K, Cao Y, Zhang J, Xu J, Hernandez SH, Wei X, Fan M (2020) Transcriptomic and metabolomic analyses reveal antibacterial mechanism of astringent persimmon tannin against Methicillin-resistant *Staphylococcus aureus* isolated from pork. *Food Chem* 309:125692
- Luo Q, Shi M, Ren Y, Gao H (2014) Transcription factors FabR and FadR regulate both aerobic and anaerobic pathways for unsaturated fatty acid biosynthesis in *Shewanella oneidensis*. *Front Microbiol* 5:736
- Lyu F, Hong YL, Cai JH, Wei QQ, Zhou X, Ding YT, Liu ZF, Liu L (2018) Antimicrobial effect and mechanism of cinnamon oil and gamma radiation on *Shewanella putrefaciens*. *J Food Sci Technol* 55:3353–3361
- Mace S, Cardinal M, Jaffres E, Cornet J, Lalanne V, Chevalier F, Serot T, Pilet MF, Dousset X, Joffraud JJ (2014) Evaluation of the spoilage potential of bacteria isolated from spoiled cooked whole tropical shrimp (*Penaeus vannamei*) stored under modified atmosphere packaging. *Food Microbiol* 40:9–17
- Mittal A, Kadyan P, Gahlaut A, Dabur R (2013) Nontargeted identification of the phenolic and other compounds of *Saraca asoca* by high performance liquid chromatography-positive electrospray ionization and quadrupole time-of-flight mass spectrometry. *ISRN Pharm* 2013:293935
- Nakayama M, Shimatani K, Ozawa T, Shigemune N, Tsugukuni T, Tomiyama D, Kurahachi M, Nonaka A, Miyamoto T (2013) A study of the antibacterial mechanism of catechins: Isolation and identification of *Escherichia coli* cell surface proteins that interact with epigallocatechin gallate. *Food Control* 33:433–439
- Ning Y, Yan A, Yang K, Wang Z, Li X, Jia Y (2017) Antibacterial activity of phenyllactic acid against *Listeria monocytogenes* and *Escherichia coli* by dual mechanisms. *Food Chem* 228:533–540
- Pang D, Liao S, Wang W, Mu L, Li E, Shen W, Liu F, Zou Y (2019) Destruction of the cell membrane and inhibition of cell phosphatidic acid biosynthesis in *Staphylococcus aureus*: an explanation for the antibacterial mechanism of morusin. *Food Funct* 10:6438–6446
- Petek M, Baebler S, Kuzman D, Rotter A, Podlesek Z, Gruden K, Ravnikar M, Urleb U (2010) Revealing fosfomycin primary effect on *Staphylococcus aureus* transcriptome: modulation of cell envelope biosynthesis and phosphoenolpyruvate induced starvation. *BMC Microbiol* 10:159
- Rees DC, Johnson E, Lewinson O (2009) ABC transporters: the power to change. *Nat Rev Mol Cell Biol* 10:218–227
- Ren X, An P, Zhai X, Wang S, Kong Q (2019) The antibacterial mechanism of pterostilbene derived from xinjiang wine grape: A novel apoptosis inducer in *Staphylococcus aureus* and *Escherichia coli*. *LWT-Food Sci Technol* 101:100–106
- Sae-leaw T, Benjakul S (2019) Prevention of quality loss and melanosis of pacific white shrimp by cashew leaf extracts. *Food Control* 95:257–266
- Shen S, Zhang T, Yuan Y, Lin S, Xu J, Ye H (2015) Effects of cinnamaldehyde on *Escherichia coli* and *Staphylococcus aureus* membrane. *Food Control* 47:196–202
- Sun D, Zhang W, Mou Z, Chen Y, Guo F, Yang E, Wang W (2017) Transcriptome analysis reveals silver nanoparticle-decorated quercetin antibacterial molecular mechanism. *ACS Appl Mater Interfaces* 9:10047–10060
- Xiang Q, Kang C, Niu L, Zhao D, Li K, Bai Y (2018) Antibacterial activity and a membrane damage mechanism of plasma-activated water against *Pseudomonas deceptionensis* CM2. *LWT-Food Sci Technol* 96:395–401
- Xu F, Wang C, Wang H, Xiong Q, Wei Y, Shao X (2018) Antimicrobial action of flavonoids from *Sedum aizoon L.* against lactic acid bacteria *in vitro* and in refrigerated fresh pork meat. *J Funct Food* 40:744–750
- Xu T, Wang Z, Lei T, Lv C, Wang J, Lu J (2015) New flavonoid glycosides from *Sedum aizoon L.* *Fitoterapia* 101:125–132
- Yang SP, Xie J, Qian YF (2017) Determination of spoilage microbiota of pacific white shrimp during ambient and cold storage using next-generation sequencing and culture-dependent method. *J Food Sci* 82:1178–1183
- Ye J, Yang S, Qian Y, Xie J (2019) Effect of cell-free supernatant from *Aeromonas sobria* on the spoilage of *Shewanella putrefaciens* in pacific white shrimp (*Litopenaeus vannamei*) with the influence of temperature fluctuation. *Appl Sci* 9:587
- Yi L, Li X, Luo L, Lu Y, Yan H, Qiao Z, Lü X (2018) A novel bacteriocin BMP11 and its antibacterial mechanism on cell envelope of *Listeria monocytogenes* and *Cronobacter sakazakii*. *Food Control* 91:160–169
- Zhang F, Zhu J, Wang H (2016) Inhibitory activity of tea polyphenols on biofilm development of *Shewanella putrefaciens*. *J Food Process Preserv* 40:910–917

Zhang X, Wu Z, Weng P (2014) Antioxidant and hepatoprotective effect of (-)-epigallocatechin 3-*O*-(3-*O*-methyl) gallate (EGCG3''Me) from Chinese oolong tea. *J Agric Food Chem* 62:10046–10054

Publisher's Note Springer Nature remains neutral with regard to jurisdictional claims in published maps and institutional affiliations.

Affiliations

Jing Wang¹ · Zongyu Chi¹ · Ke Zhao¹ · Hongfei Wang¹  · Xin Zhang¹ · Feng Xu¹ · Xingfeng Shao¹ · Yingying Wei¹

✉ Hongfei Wang
wanghongfei@nbu.edu.cn

✉ Xin Zhang
zhangxin@nbu.edu.cn

Jing Wang
wanghongfei@nbu.edu.cn

¹ Department of Food Science and Engineering, College of Food and Pharmaceutical Science, Ningbo University, Ningbo 315211, Zhejiang, People's Republic of China